PHYSICAL REVIEW B VOLUME 24, NUMBER 10 15 NOVEMBER 1981

Four-wave mixing and phase conjugation near the band edge

A. Elçi
Max-Planck-Institut für Quantenoptik, D-8046 Garching, Munich, Federal Republic of Germany

D. Rogovin
Science Applications, Inc., 1200 Prospect Street, La Jolla, California 92038
(Received 22 December 1980)

We discuss degenerate four-wave mixing and phase conjugation near the band edge of direct-gap semiconductors and show that the reflectivity for conjugate waves is enhanced in the vicinity of the band edge. We also compare the quantum-mechanical results with the classical Drude model.

I. INTRODUCTION

There is at present a considerable body of work on phase conjugation via degenerate four-wave mixing in semiconductors.[1-6] It has been motivated partly by the availability of a variety of frequency ranges, and partly by the relatively high efficiencies observed in these materials. This paper, too, is concerned with degenerate four-wave mixing. We consider a direct-gap semiconductor and calculate the contribution of interband transitions near the band edge to the third-order susceptibility $\chi^{(3)}(\omega=\omega+\omega-\omega)$. We also consider the absorption coefficient α in the semiconductor in order to obtain a realistic expression for the conjugate wave reflectivity η.

There are two reasons for the interest in a band-edge mechanism for four-wave mixing. First, $\chi^{(3)}$ is enhanced as $\hbar\omega$ increases to E_G, the band gap. As a result, η is also enhanced despite increased absorption (which adversely affects phase conjugation[7,8]). Second, a band-edge mechanism offers a greater potential for frequency tunability, since in many semiconductor compounds such as $Ga_{1-x}(InAs)_x$, $Cd_{1-x}(HgTe)_x$, $Pb_{1-x}(SnSe)_x$, etc. E_G can be continuously varied by changing composition.[9]

A number of authors have discussed band-edge mechanisms for four-wave mixing.[1,3,6] Among these, Jain *et al.*[1,3] have considered a mechanism which is similar to what we have in mind. They imagine creation of an electron-hole plasma in the semiconductor and use a Drude model to calculate $\chi^{(3)}$. In this paper, however, we perform a density matrix calculation to provide a more precise picture of the frequency dependence of $\chi^{(3)}$ and η. Also, our results apply to frequencies that are lower than E_G. A detailed comparison of our results with those of Ref. 1 is given in Sec. V. Finally, we also note that Khan *et al.*[4] have studied a case in which $\chi^{(3)}$ is resonant for $\hbar\omega\sim E_G$ because of a nonparabolic band structure. This nonlinear process is quite different than the one discussed here.[10] Here, we are concerned with an ordinary and direct electron-field coupling via interband transitions.

In Sec. II, we describe the band structure used in the calculation. It is a simplified version of the band structure of III-V compounds, chosen with the phase conjugation of iodine laser beams in mind. In Sec. III we give the general results for a two-component plasma in the semiconductor. In Sec. IV, the general results are specialized to small perturbations from thermal equilibrium. Finally, in Sec. VI, we discuss the reflectivity of a specific direct-gap semiconductor, $Ga_{1-x}(InAs)_x$.

The main result of our work is that the reflectivity of conjugate waves has a peak in the vicinity of the band edge, and below the band gap, the reflectivity scales as the absorption coefficient when the frequency is varied. The precise position of the peak depends parametrically on the sample thickness. The peak shifts to lower frequencies for thicker samples, as one might expect from the depletion of the pump waves. If the depletion of the pump waves is negligible, as when the semiconductor is saturated, then the reflectivity is nearly constant above the band edge and decreases rapidly below it, independently of the sample thickness.

II. BAND MODEL

To be definite, we assume a band structure as shown in Fig. 1, which is typical of III-V com-

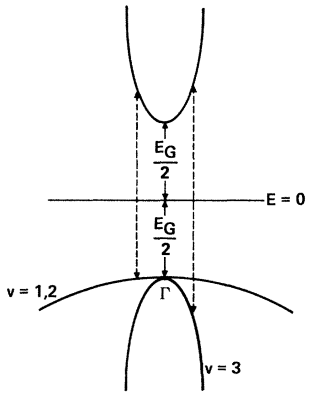

FIG. 1. Model band structure.

pounds. It has one light-hole band, two heavy-hole bands which are degenerate, and one conduction band. To simplify the calculation we also assume that the bands are parabolic:

$$E_c(\vec{k})=(E_G/2)+(\hbar^2k^2/2m_c^*) \tag{1a}$$

$$E_v(\vec{k})=-(E_G/2)-(\hbar^2k^2/2m_v^*) \tag{1b}$$

$$(v=1,2,3)\ ,$$

where the m^*'s are the appropriate effective masses near the center of the Brillouin zone (BZ). For the calculation one also needs the dipole matrix element for the interband transitions. It is related to the more familiar interband momentum matrix element by the following relations:

$$\vec{\mu}=-e\epsilon_\infty^{-1/2}\vec{x}\ , \tag{2a}$$

$$\vec{p}=-im_0\hbar^{-1}[\vec{x},H_0]\ , \tag{2b}$$

$$\vec{\mu}_{cv}=-ie\hbar m_0^{-1}\epsilon_\infty^{-1/2}(E_c-E_v)^{-1}\vec{p}_{cv}\ . \tag{2c}$$

Here ϵ_∞ is the high-frequency dielectric constant, m_0 is the bare electron mass, and H_0 is the one-electron crystal Hamiltonian. The factor $\epsilon_\infty^{-1/2}$ in (2a) comes from high-frequency screening of electrons and renormalizes the bare electronic charge. Since our concern is with the band edge, the right-hand side of (2c) need be evaluated only at $\vec{k}=0$. $\vec{\mu}_{cv}$ can be taken as constant.

We are interested in those situations in which the semiconductor is either at room temperature or at a temperature which is not too low relative to room temperature. At these temperatures the absorption edge is smoothly broadened to frequencies which are considerably below the band edge, due to phonons and the presence of excitonic states. At room temperatures, individual excitonic states are not observable as they are smeared into a continuum. To take into account this broadening as well as the relaxation of the carriers, we assign average linewidths γ_c and γ_v to electron and hole states, respectively. Although γ_c and γ_v are energy dependent, this procedure should be valid as long as most of the carriers are confined to near the band edge. Another parameter at one's disposal to model correctly the Coulombic effects on the band edge is the band gap. If need be, one may use an effective gap in the final results. Finally, one can justify the whole procedure by looking at the absorption coefficient calculated from the model. In all the cases we considered, the calculated coefficient reproduces the overall features of the experimentally observed curves with reasonable linewidths at room temperatures. For lower temperatures, there are well-defined discrete excitonic peaks and one must take the discrete nature of these peaks into account. This requires considerable modification of the calculation and is reserved for another publication.

III. THIRD-ORDER SUSCEPTIBILITY, ABSORPTION, AND REFLECTIVITY

The geometry of degenerate four-wave mixing is shown in Fig. 2. We assume that all four waves are linearly polarized in the z direction and actually calculate $\chi^{(3)}_{zzzz}(\omega=\omega+\omega-\omega)$. Since absorption is important for phase conjugation, we also calculate the frequency-dependent absorption coefficient $\alpha(\omega)$ under the same assumptions. A density matrix calculation gives the following expressions for $\chi^{(3)}$ and α (see Refs. 8 and 11):

$$\chi^{(3)}=\sum_{v=1}^{3}\int_{BZ}d\vec{k}(2\pi)^{-3}\,|\mu_{cv}^z|^4[f(E_v)-f(E_c)]$$

$$\times[(\gamma_c+\gamma_v)^2(\gamma_c\gamma_v)^{-1}(L_{vc}-L_{cv})(|L_{vc}|^2+|L_{cv}|^2)$$

$$+(4\hbar\omega+i\gamma_c+i\gamma_v)(2\hbar\omega+i\gamma_c)^{-1}(2\hbar\omega+i\gamma_v)^{-1}(L_{cv}^2-L_{vc}^2)]\ , \tag{3a}$$

$$\alpha=\hbar n\omega^2(c\pi^2E_G)^{-1}\sum_{v=1}^{3}\gamma_{cv}\,|\,\mu_{cv}^z\,|^2\int_{\mathrm{BZ}}d\vec{k}[\mathcal{f}(E_v)-\mathcal{f}(E_c)](\,|\,L_{cv}\,|^2+|\,L_{vc}\,|^2)\,, \tag{3b}$$

where $n=\sqrt{\epsilon_\infty}$ is the index of refraction, and

$$L_{nn'}=[\hbar\omega-E_n(\vec{k})+E_{n'}(\vec{k})+i\gamma_{nn'}]^{-1}\,, \tag{4a}$$

$$\gamma_{nn'}=(\gamma_n+\gamma_{n'})/2\,, \tag{4b}$$

$$\mathcal{f}(E_n)=(1+\exp\{\beta[E_n(\vec{k})-E_{Fn}]\})^{-1}\,,\qquad \beta=(k_BT)^{-1}\,, \tag{4c}$$

$$E_{Fn}=\begin{cases}E_{Fc} & \text{for } n=c\\ -E_{Fh} & \text{for } n=v=1,2,3\,.\end{cases} \tag{4d}$$

In (4c) and (4d) E_{Fn} are Fermi energies for electrons and holes, assumed to be distinct in order to include those situations in which absorption at $\hbar\omega$ significantly affects band populations.[12]

One can let the upper limit of k go to infinity to simplify the integrals. We do not expect much error resulting from this procedure since as $k\to\infty$, the integrands decrease rapidly for parabolic bands. However, the situation is quite different for nonparabolic bands. For instance, the integrals for Kane's two-band model[13] diverge if one lets the upper limit of k go to infinity; therefore, they must be evaluated for a finite Brillouin zone.

$\chi^{(3)}$ and α consist of two types of terms,

$$\chi^{(3)}=\sum_{v=1}^{3}(K_v^0+K_v^t)\,, \tag{5a}$$

$$\alpha=\sum_{v=1}^{3}(A_v^0+A_v^t)\,, \tag{5b}$$

where K_v^0 and A_v^0 are temperature independent, and K_v^t and A_v^t are temperature dependent. This separation is effected by writing the population factor as

$$\begin{aligned}&\mathcal{f}(E_v)-\mathcal{f}(E_c)\\ &\quad=1-[1-\mathcal{f}(E_v)+\mathcal{f}(E_c)]\\ &\quad=1-(\{1+\exp[\beta(-E_v-E_{Fh})]\}^{-1}\\ &\qquad+\{1+\exp[\beta(E_c-E_{Fc})]\}^{-1})\,.\end{aligned} \tag{6}$$

The integrals for K_v^0 and A_v^0 can be evaluated by contour integration (see the Appendix) and one finds

$$\begin{aligned}K_v^0=(2\pi)^{-1}\hbar^{-3}m_v^{3/2}\,|\,\mu_{cv}^z\,|^4\{&[2\gamma_{cv}^2(\gamma_c\gamma_v\hbar\omega\sqrt{\Delta_-})^{-1}]\\ &+[(\Delta_-+i\gamma_{cv})(\Omega_-\sqrt{\Delta_-})^{-1}][\gamma_{cv}^2(\Delta_-\gamma_c\gamma_v)^{-1}+(4\hbar\omega+2i\gamma_c)^{-1}+(4\hbar\omega+2i\gamma_v)^{-1}]\\ &+[(\Delta_+-i\gamma_{cv})(\Omega_+\sqrt{\Delta_+})^{-1}][\gamma_{cv}^2(\Delta_+\gamma_c\gamma_v)^{-1}-(4\hbar\omega+2i\gamma_c)^{-1}-(4\hbar\omega+2i\gamma_v)^{-1}]\\ &-[2\gamma_{cv}^2(\gamma_c\gamma_v\hbar\omega\sqrt{\Delta_+})^{-1}]\}\end{aligned} \tag{7a}$$

and

$$A_v^0=4n\omega^2m_v^{3/2}\,|\,\mu_{cv}^z\,|^2(\hbar^2cE_G)^{-1}[\Delta_-+2(\hbar\omega-E_G)]^{1/2}\,, \tag{7b}$$

where

$$m_v=m_c^*m_v^*(m_c^*+m_v^*)^{-1}\,, \tag{7c}$$

$$\Omega_\pm=[(E_G\pm\hbar\omega)^2+\gamma_{cv}^2]^{1/2}\,, \tag{7d}$$

and

$$\Delta_\pm=\Omega_\pm+(E_G\pm\hbar\omega)\,. \tag{7e}$$

The temperature-dependent terms cannot be evaluated explicitly for arbitrary temperature. We write them in terms of Fermi-Dirac integrals of the dimensionless form

$$F_m^n(j;a)=\int_0^\infty dy\,y^n(y^2+a)^{-m}[1+c_j\exp(b_jy^2)]^{-1}\,. \tag{8}$$

Let us define

$$\zeta=(E_G+i\gamma_{cv})/\hbar\omega \ , \tag{9a}$$

$$c_1=\exp[\beta(E_G/2-E_{Fc})] \ , \tag{9b}$$

$$c_2=\exp[\beta(E_G/2-E_{Fh})] \ , \tag{9c}$$

$$b_1=(m_v/m_c^*)\beta\hbar\omega \ , \tag{9d}$$

$$b_2=(m_v/m_v^*)\beta\hbar\omega \ . \tag{9e}$$

K_v^t and A_v^t are then given by

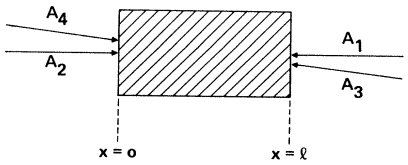

FIG. 2. Geometry of four-wave mixing. A_3 and A_4 are the amplitudes of the conjugate and signal waves, respectively. A_1 and A_2 are the amplitudes of the pump waves.

$$\begin{aligned}K_v^t=&(\pi^2\hbar^3\gamma_c\gamma_v)^{-1}(2m_v)^{3/2}(\hbar\omega)^{1/2}\,|\mu_{cv}^z|^4\\&\times\sum_{j=1}^{2}\{\mathrm{Im}[F_1^2(j;\zeta-1)+F_1^2(j;\zeta^*+1)]+i(\gamma_{cv}/\hbar\omega)[F_2^2(j;\zeta^*-1)-F_2^2(j;\zeta+1)]\\&+(\gamma_{cv}/\hbar\omega)\mathrm{Re}[i(\zeta-1)F_1^0(j;\zeta-1)+i(\zeta^*+1)F_1^0(j;\zeta^*+1)]\\&+(\gamma_c\gamma_v/2\hbar\omega)[(2\hbar\omega+i\gamma_c)^{-1}+(2\hbar\omega+i\gamma_v)^{-1}][F_2^2(j;\zeta+1)-F_2^2(j;\zeta^*-1)]\}\end{aligned} \tag{10a}$$

and

$$A_v^t=4\omega n\,|\mu_{cv}^z|^2(2m_v\omega/\hbar)^{3/2}(\pi cE_G)^{-1}\sum_{j=1}^{2}\mathrm{Im}[F_1^2(j;\zeta-1)+F_1^2(j;\zeta+1)] \ . \tag{10b}$$

Finally, the reflectivity for conjugate waves in degenerate four-wave mixing is given by[7,8]

$$\eta=|\kappa\sin\xi l\,|^2\,|\xi\cos\xi l+\alpha\sin\xi l\,|^{-2} \ , \tag{11a}$$

where

$$|\kappa|=16\pi^2\omega c^{-2}\epsilon_\infty^{-1}(I_1I_2)^{1/2}|\chi^{(3)}| \tag{11b}$$

and

$$\xi=(|\kappa|^2-\alpha^2)^{1/2} \ . \tag{11c}$$

In Eq. (11a), l is the length of the nonlinear mixing region, and I_1 and I_2 are the intensities of the two counterpropagating pump waves. We note that (11a) is derived under the assumption that the conjugate and signal waves are depleted but the pump waves are not. When the depletion of the pump waves is also taken into account, as seen from Fig. 2, the constant pump amplitudes A_1 and A_2 are replaced by

$$A_1(x)=A_1(l)\exp[-(l-x)\alpha/2] \ , \tag{11d}$$

$$A_2(x)=A_2(0)\exp(--\alpha x/2) \ , \tag{11e}$$

and thus the product

$$A_1(x)A_2(x)=A_1(l)A_2(0)\exp(-\alpha l/2) \tag{11f}$$

is independent of position. $|\kappa|$ becomes

$$|\kappa|=16\pi^2\omega c^{-2}\epsilon_\infty^{-1}(I_1I_2)^{1/2}|\chi^{(3)}|\exp(-\alpha l/2) \ . \tag{11g}$$

Above the band edge, α is usually on the order of $10^4\ \mathrm{cm}^{-1}$. All four waves can be severely depleted and one should use (11g). The use of (11b) should be restricted to frequencies that are lower than the band edge. There is still significant absorption at these frequencies, however, due to the broadening of the absorption edge, and the depletion of the signal and conjugate waves should be taken into account even when the depletion of the pump waves is not.

IV. MODERATE EXCITATIONS

In order to obtain efficient phase conjugation, one would naturally seek a situation in which absorption at $\hbar\omega$ is as low as possible. We now take this to be the case and assume that electron and hole populations are not perturbed significantly from their equilibrium forms. We note in passing that this assumption contrasts with the premise of Ref. 1 in which Jain and Klein imagine creation of a dense electron-hole plasma in the semiconductor.

In their case, it would be more appropriate to assign a separate Fermi energy to each component of the plasma, since each thermalizes separately before the interband transitions can take over and bring the two components into a common thermal equilibrium.[12]

At the thermal equilibrium, there is one common Fermi energy:

$$E_F = E_{Fc} = -E_{Fh} \simeq (k_B T/2)\ln\left[1+\sum_v (m_v^*/m_c^*)^{3/2}\right] . \quad (12)$$

One can therefore set

$$c_1 \simeq c_2 \simeq \exp(\beta E_G/2) >> 1 \quad (13)$$

for band gaps on the order of 0.5–1 eV and for room temperatures. Also, the integrand in (8) contributes mostly in the vicinity of $y=0$ and

$$F_m^n(j;a) \approx (2c_j)^{-1} a^{-m} b_j^{-(n+1)/2} \Gamma\left[\frac{n+1}{2}\right] . \quad (14)$$

To simplify the following discussion, we further assume that $\gamma_c = \gamma_v = \gamma$ and focus our attention on the vicinity of the band edge, by which we mean $|E_G - \hbar\omega|/E_G << 1$. In the vicinity of the band edge (7a), (7b), and (14) yield

$$\sum_v K_v^0 = \chi_0[i+\delta+(1+\delta^2)^{1/2}] \times [\delta+(1+\delta^2)^{1/2}]^{-3/2}(1+\delta^2)^{-1/2} , \quad (15a)$$

$$\sum_v K_v^t = \chi_t(\delta+1)(\delta+i)(1+\delta^2)^{-2} , \quad (15b)$$

$$\sum_v A_v^0 = \alpha_0[(1+\delta^2)^{1/2}-\delta]^{1/2} , \quad (15c)$$

and

$$\sum_v A_v^t = \alpha_t(1+\delta^2)^{-2} , \quad (15d)$$

where

$$\delta = (E_G - \hbar\omega)/\gamma , \quad (16a)$$

$$\chi_0 = (2\pi\hbar^3\gamma^{3/2})^{-1} \sum_v m_v^{3/2} |\mu_{cv}^z|^4 , \quad (16b)$$

$$\chi_t = 2(i-1)(2\pi\beta)^{-3/2}\hbar^{-3}\gamma^{-3}\exp(-\beta E_G/2) \times \sum_v |\mu_{cv}^z|^4 [(m_c^*)^{3/2}+(m_v^*)^{3/2}] , \quad (16c)$$

$$\alpha_0 = 4n\omega^2\gamma^{1/2}(\hbar^2 c E_G)^{-1} \sum_v m_v^{3/2} |\mu_{cv}^z|^2 , \quad (16d)$$

and

$$\alpha_t = -4n(2\pi\hbar)^{-1/2}(cE_G\gamma)^{-1}\omega^{7/2}\exp(-\beta E_G/2) \times \sum_v |\mu_{cv}^z|^2 [(m_c^*)^{3/2}+(m_v^*)^{3/2}] . \quad (16e)$$

To compare the temperature-dependent and -independent terms, note that

$$|\chi_t/\chi_0| \sim (2\pi)(k_B T/\pi\gamma)^{3/2}\exp(-\beta E_G/2) \quad (17a)$$

and

$$|\alpha_t/\alpha_0| \sim (2\pi)(\hbar\omega/2\pi\gamma)^{3/2}\exp(-\beta E_G/2) . \quad (17b)$$

Owing to the exponential terms, the temperature-dependent terms are clearly negligible either for room temperatures under thermal equilibrium conditions, or for small perturbations from thermal equilibrium. For lower temperatures they decrease further, exponentially. Thus, for all intents and purposes, $\chi^{(3)}$ and α are given by the temperature-independent terms under moderate excitations as long as the band gap is not too small:

$$\chi^{(3)} = \chi_0[i+\delta+(1+\delta^2)^{1/2}] \times [\delta+(1+\delta^2)^{1/2}]^{-3/2}(1+\delta^2)^{-1/2} , \quad (18a)$$

$$\alpha = \alpha_0[(1+\delta^2)^{1/2}-\delta]^{1/2} . \quad (18b)$$

Finally one needs $|\chi^{(3)}|$ for the reflectivity:

$$|\chi^{(3)}| = \sqrt{2}\chi_0(1+\delta^2)^{-1/4}[(1+\delta^2)^{1/2}+\delta]^{-1} . \quad (19)$$

Figure 3 shows $|\chi^{(3)}|/(\sqrt{2}\chi_0)$ as a function of δ, the frequency detuning per linewidth.

Equations (18) and (19) predict an interesting behavior for the reflectivity. Let us ignore the pump depletion for a moment. Under usual operating conditions ξ of Eq. (11c) is imaginary and (11a) simplifies to

$$\eta \simeq |\kappa|^2(2\alpha)^{-2} \propto |\chi^{(3)}|^2\alpha^{-2} . \quad (20a)$$

Below the band gap, $\delta >> 1$ and

$$|\chi^{(3)}| \simeq 2\chi_0(2\delta)^{-3/2} , \quad (20b)$$

$$\alpha \simeq \alpha_0(2\delta)^{-1} , \quad (20c)$$

and thus

$$\eta \propto \alpha . \quad (20d)$$

As a result, below the band gap, the reflectivity

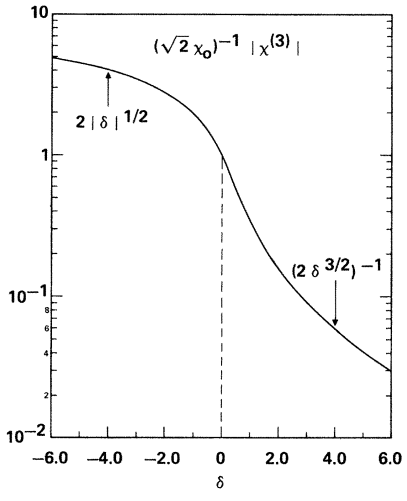

FIG. 3. $|\chi^{(3)}(\omega=\omega+\omega-\omega)|$ as a function of the frequency detuning per linewidth.

scales as the absorption coefficient. On the other hand, above the band gap, $\delta<0$, $|\delta|>>1$, and

$$|\chi^{(3)}|\simeq 2\chi_0(2\delta)^{1/2}\,, \tag{20e}$$

$$\alpha\simeq\alpha_0(2\delta)^{1/2}\,, \tag{20f}$$

and η is constant as long as the conditions under which (20a) is true hold.

V. COMPARISON WITH THE DRUDE MODEL

We now compare our expression for $\chi^{(3)}$ with that of Jain and Klein.[1] Their expression for $\chi^{(3)}$, obtained from a Drude model, is

$$\chi_D^{(3)}=nce^2\tau\eta^*\alpha^*(8\pi m_{eh}^*\hbar\omega^3)^{-1}\,. \tag{21}$$

Here τ is the lifetime for electrons and holes, α^* is the total absorption coefficient, $\eta^*\alpha^*$ designates the fraction of the absorption which corresponds to an actual electron-hole pair creation (i.e., $\eta^*\alpha^*$ corresponds to our α), and m_{eh}^* is the reduced mass of an electron and a hole: $m_{eh}^*=m_e^*m_h^*(m_e^*+m_h^*)^{-1}$. $\chi_D^{(3)}$ is real and describes an adiabatic response of the system. It corresponds to our $\mathrm{Re}\chi^{(3)}$. Our expression for $\chi^{(3)}$ has an additional part which is imaginary. $\mathrm{Im}\chi^{(3)}$ describes those processes in which at least one real transition occurs. Note that above the band edge, $\delta<0$ and $|\delta|>>1$. One therefore has $\alpha>>\alpha_0$, and

$$\mathrm{Im}\chi^{(3)}\simeq(2\chi_0/\alpha_0)\alpha\,. \tag{22}$$

Thus, above the band edge, $\mathrm{Im}\chi^{(3)}$ is proportional to the absorption coefficient, having the same functional dependence on the frequency detuning $(E_G-\hbar\omega)$ as α. This is consistent with having at least one real transition occur.

To compare $\chi_D^{(3)}$ and $\mathrm{Re}\chi^{(3)}$, we make the following approximations. The ratio of the sums over the dipole moments can be estimated as

$$\left[\sum_v m_v^{3/2}|\mu_{cv}^z|^4\right]\left[\sum_v m_v^{3/2}|\mu_{cv}^z|^2\right]^{-1}\simeq|\mu_{c1}^z|^2\,. \tag{23}$$

Using (2c), one has

$$|\mu_{c1}^z|^2=e^2\hbar^2|P_{c1}^z|^2(m_0^2n^2E_G^2)^{-1}\,. \tag{24}$$

The momentum matrix element is related to the electron and hole masses near the band edge (see Ref. 12):

$$|P_{c1}^z|^2(m_0^2E_G)^{-1}\approx(2m_{eh}^*)^{-1}\,. \tag{25}$$

With these approximations and also using $\gamma=(\hbar/\tau)$, one finds

$$\mathrm{Re}\chi^{(3)}\approx(\hbar\omega/2)[(\hbar\omega-E_G)^2+\gamma^2]^{-1/2}n^{-4}\chi_D^{(3)}\,. \tag{26}$$

Thus, as far as the frequency dependence is concerned, the two expressions differ only by the square root of a Lorentz factor. The other factor n^{-4} arises from two sources. One is that we are taking into account the short-wavelength screening and treating electrons as particles each with an effective charge $e/\sqrt{\epsilon_\infty}=e/n$, as in (2a). This contributes a factor n^{-2} in (26). The remaining n^{-2} factor comes from the difference between the way we count the number of photons and the way it is done in Ref. 1. We use the standard expansion for the electric field operator such that (see Ref. 14)

$$\vec{\mathrm{E}}(\vec{x},t)=\sum_\lambda i(2\pi\hbar\omega_\lambda/V)^{1/2}\hat{e}_\lambda \times\{b_\lambda\exp[i(\vec{k}_\lambda\cdot\vec{x}-\omega_\lambda t)] -b_\lambda^\dagger\exp[-i(\vec{k}_\lambda\cdot\vec{x}-\omega_\lambda t)]\}\,, \tag{27}$$

with the photon current density given by

$$j_\gamma=c\langle\vec{\mathrm{E}}^2\rangle_\omega(4\pi\hbar\omega n)^{-1}\,. \tag{28}$$

For complex field amplitudes,

$$j_\gamma=c\langle\vec{\mathrm{E}}\cdot\vec{\mathrm{E}}^*\rangle_\omega(8\pi\hbar\omega n)^{-1}\,. \tag{29}$$

This expression for j_γ differs from the correspond-

ing one in Ref. 1 in that (29) has an extra n^{-2} factor. Finally, if we write out $n^{-4}\chi_D^{(3)}$,

$$n^{-4}\chi_D^{(3)}=(c/n)(e^2/\epsilon_\infty)(\tau\eta^*\alpha^*)(8\pi m_{eh}^*\hbar\omega^3)^{-1}\ , \tag{30}$$

we see that n^{-4} factor helps to renormalize both the charge and the speed of light. It is interesting that the presence of n^{-4} somewhat compensates for the Lorentz factor in (26) and makes $\mathrm{Re}\chi^{(3)}$ and $\chi_D^{(3)}$ comparable, since usually $n^2\sim 10-20$ for semiconductors.

VI. REFLECTIVITY FOR $Ga_{1-x}(InAs)_x$

We now consider a specific semiconductor $Ga_{1-x}(InAs)_x$ with $x\simeq 0.4$ for which the band gap is $E_G\simeq 0.95$ eV. This choice is motivated by the fact that $\lambda_0=2\pi\hbar c E_G^{-1}\simeq 1.3$ μm, which coincides with the wavelength of high-energy iodine lasers. There has been a practical interest in obtaining phase conjugation at the iodine wavelength. To the authors knowledge there is no gaseous or atomic system which matches this wavelength and which might be used for resonant enhancement of the conjugation process. Neutral iodine itself cannot be used, since the lasting transition is a magnetic dipole transition. A semiconductor such as $Ga_{1-x}(InAs)_x$ is, therefore, a natural choice for phase conjugation at $\lambda_0=1.3$ μm.

The remaining parameters for our sample are $\epsilon_\infty\simeq 10$, $m_c^*=m_3^*\simeq 0.1m_0$, and $m_1^*=m_2^*\simeq 0.6m_0$ (see Ref. 15). A typical lifetime is $\tau=\hbar/\gamma\simeq 10^{-11}$ sec^{-1}. Thus,

$$m_{eh}^*=m_c^*m_1^*(m_c^*+m_1^*)^{-1}\simeq 0.09m_0 \tag{31a}$$

and

$$|\mu_{c1}^z|\approx e\hbar(2m_{eh}^*\epsilon_\infty E_G)^{-1}\simeq 10\ \mathrm{D}\ , \tag{31b}$$

where we used (24) and (25). Setting $E_G\simeq\hbar\omega$ in (16b) and (16d) yields $\chi_0\approx 3\times 10^{-6}$ esu and $\alpha_0\approx 1.2\times 10^3$ cm^{-1}. The value of α_0, which corresponds to the value of α at the exact band edge $\delta=0$, is in reasonable agreement with the experimentally observed value for GaAs (see page 61 of Ref. 15). Further, let $I_1=I_2=1$ MW/cm^2, then from (11b), $|\kappa|\approx 1.1\times 10^3$ cm^{-1}, which is comparable to but less than α. Note that $|\chi^{(3)}|$ and hence $|\kappa|$ are quite sensitive to the linewidth. For example, for $\tau=10^{-12}$ sec^{-1}, one finds $\alpha_0\approx 4\times 10^3$ cm^{-1}, $\chi_0\approx 10^{-7}$ esu, and $|\kappa|\approx 36$ cm^{-1}. As mentioned earlier the parameter ξ is usually an imaginary quantity, and

$$\eta=|\kappa|^2(2\alpha)^{-2}\ . \tag{32}$$

Thus, if the pump waves are not depleted and $\tau=10^{-11}$ sec^{-1}, one has from (32) and (11b) that $\eta\simeq 0.22=22\%$, which is a reasonably efficient phase conjugation.

The frequency-detuning dependence of η as given by (32) can be written out as

$$\eta=\eta_0(1+\delta^2)^{-1/2}[(1+\delta^2)^{1/2}-\delta]\times\exp\{-\rho_0[(1+\delta^2)^{1/2}-\delta]^{1/2}\}\ , \tag{33a}$$

where

$$\eta_0=2\pi^2E_G^2(\hbar^2\omega^2c^2\gamma^4n^6)^{-1}\times\left[\sum_v m_v^{3/2}|\mu_{cv}^z|^4\right]^2\left[\sum_v m_v^{3/2}|\mu_{cv}^z|^2\right]^{-2}I_1I_2 \tag{33b}$$

and

$$\rho_0=\alpha_0 l\ . \tag{33c}$$

We used (11g) to obtain (33a). The parameter ρ_0 may be called the optical thickness of the sample. If one wants to ignore the pump depletion, one can do so by letting $\rho_0\to 0$ in (33a), which would then revert to the form that is obtained from (11b). Figure 4 shows η/η_0 versus δ for various ρ_0. Above the band edge,

$$\eta/\eta_0\simeq 2[1-(4\delta^2)^{-1}]\exp[-\rho_0(2|\delta|)^{1/2}]\ . \tag{34a}$$

Thus, when the pump waves are undepleted, η has

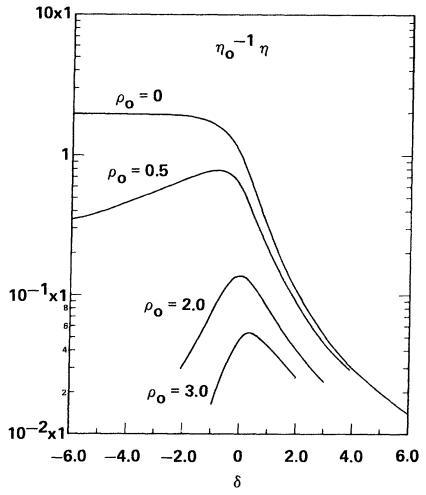

FIG. 4. Reflectivity of conjugate waves as a function of the frequency detuning for various optical thicknesses.

an upper limit which is $2\eta_0$ for frequency detunings that are large relative to the linewidth. For the specific semiconductor above and for $I_1=I_2=1$ MW/cm^2 and $\tau=10^{-11}$ sec, $2\eta_0\simeq 0.44=44\%$. Similarly, below the band edge,

$$\eta/\eta_0\simeq(2\delta^2)^{-1}\exp(-\rho_0/\sqrt{2\delta}) , \tag{34b}$$

which decreases rapidly with increasing δ.

It is clear that the optimum place for phase conjugation is in the vicinity of the band edge. When the pump depletion is taken into account, there is more structure in the reflectivity as a function of the frequency detuning. Also, the reflectivity decreases as $\hbar\omega-E_G$ increases above the band edge. The reflectivity generally peaks in the vicinity of the band edge. The position of the peak is given by a fifth-order equation which is obtained by setting the derivative of η/η_0 with respect to δ equal to zero:

$$y^5+y-4/\rho_0=0 , \tag{35a}$$

where

$$y\equiv[(1+\delta^2)^{1/2}-\delta]^{1/2} . \tag{35b}$$

Since y^5+y is a monotomically increasing function, there is only one real root and there is only one peak in the reflectivity. As ρ_0 increases, the peak shifts to larger δ. It follows that if the semiconductor is saturated, the optimum place for phase conjugation is slightly above the band edge, and if there is significant absorption at ω, the place to be is slightly below the band edge.

ACKNOWLEDGMENT

We gratefully acknowledge the support of AFOSR for this work.

APPENDIX

For the convenience of the reader, we explicitly display the contour integrations which yield (7a) and (7b). After the angular integrations are performed, one obtains four types of integrals which can be written as

$$I_1(A)=\int_{-\infty}^{+\infty} dy\, y^2(y^2+A)^{-2}(y^2+A^*)^{-1} , \tag{A1}$$

$$I_2(A,B)=\int_{-\infty}^{+\infty} dy\, y^2(y^2+A)^{-1}(y^2+B)^{-1}\times(y^2+B^*)^{-1} , \tag{A2}$$

$$I_3(A)=\int_{-\infty}^{+\infty} dy\, y^2(y^2+A)^{-2} , \tag{A3}$$

$$I_4(A,B)=\int_{-\infty}^{+\infty} dy\, y^2[(y^2+A)^2+B^2]^{-1} . \tag{A4}$$

The integrand of I_1 can be written as

$$\begin{aligned} y^2(y^2+A)^{-2}(y^2+A^*)^{-1} &= A(A-A^*)^{-2}(y^2+A)^{-1} \\ &\quad -A^*(A-A^*)^{-2}(y^2+A^*)^{-1} \\ &\quad -(A-A^*)^{-1}y^2(y^2+A)^{-2} . \end{aligned} \tag{A5}$$

An integration by parts gives

$$\int_{-\infty}^{+\infty} dy\, y^2(y^2+A)^{-2}=2^{-1}\int_{-\infty}^{+\infty} dy(y^2+A)^{-1} . \tag{A6}$$

Thus,

$$\begin{aligned} I_1(A)=2^{-1}(A-A^*)^{-2} &\times\left[(A+A^*)\int_{-\infty}^{+\infty} dy(y^2+A)^{-1}\right. \\ &\left.-2A^*\int_{-\infty}^{+\infty} dy(y^2+A^*)^{-1}\right] . \end{aligned} \tag{A7}$$

Let $A=a^2e^{2i\phi}$, where a is real and positive and $-\pi/2\le\phi\le\pi/2$. There are two distinct roots for $y^2+A=0$, which are $y_0=a\exp[i(\phi+\pi/2)]$ and $y_1=a\exp[i(\phi+3\pi/2)]$. Closing the contour in the upper half,

$$\begin{aligned} \int_{-\infty}^{+\infty} dy(y^2+A)^{-1} &= (\pi/a)\exp(-i\phi) \\ &= \pi(1+A^*/|A|) \\ &\quad\times(2|A|+A+A^*)^{-1/2} . \end{aligned} \tag{A8}$$

Using (A8) in (A7), one finds that

$$\begin{aligned} I_1(A) &= (\pi/4a^3)(1+\cos2\phi)^{-1}\exp(-i\phi) \\ &= (\pi/2)(1+A^*/|A|)(2|A|+A+A^*)^{-3/2} . \end{aligned} \tag{A9}$$

The integrand of I_2 can be written as

$$\begin{aligned} y^2(y^2+A)^{-1}(y^2+B)^{-1}(y^2+B^*)^{-1} &= -A(A-B)^{-1}(A-B^*)^{-1}(y^2+A)^{-1}-B(B-A)^{-1}(B-B^*)^{-1}(y^2+B)^{-1} \\ &\quad -B^*(B^*-A)^{-1}(B^*-B)^{-1}(y^2+B^*)^{-1} . \end{aligned} \tag{A10}$$

Now use (A8):

$$I_2(A,B)=-\pi[A(1+A^*/|A|)(A-B)^{-1}(A-B^*)^{-1}(2|A|+A+A^*)^{-1/2}$$
$$+B(1+B^*/|B|)(B-A)^{-1}(B-B^*)^{-1}(2|B|+B+B^*)^{-1/2}$$
$$+B^*(1+B/|B|)(B^*-A)^{-1}(B^*-B)^{-1}(2|B|+B^*+B)^{-1/2}]$$
$$=\pi(A-B)^{-1}(A-B^*)^{-1}[(A+|B|)(2|B|+B+B^*)^{-1/2}-(A+|A|)(2|A|+A+A^*)^{-1/2}] . \tag{A11}$$

In (A3), an integration by parts yields

$$I_3(A)=2^{-1}\int_{-\infty}^{+\infty} dy(y^2+A)^{-1}=(\pi/2)(1+A^*/|A|)(2|A|+A+A^*)^{-1/2} . \tag{A12}$$

Finally, the integrand of (A4) can be written as

$$y^2[(y^2+A)^2+B^2]^{-1}=(i/2B)[(A-iB)(y^2+A-iB)^{-1}-(A+iB)(y^2+A+iB)^{-1}] , \tag{A13}$$

where A and B are real. Now using (A8) yields

$$I_4(A,B)=(\pi/B\sqrt{2})(A^2+B^2)^{1/4}[(A^2+B^2)^{1/2}-A]^{1/2} . \tag{A14}$$

Let $\mathcal{J}_0=(4\pi^2)^{-1}(2m_v/\hbar^2)^{3/2}$. Using (A7), (A11), (A12), and (A14), one finds

$$\int d\vec{k}(2\pi)^{-3}L_{vc}(\omega)|L_{vc}(\omega)|^2=\mathcal{J}_0 I_1(\hbar\omega+E_G+i\gamma_{cv}) , \tag{A15a}$$

$$\int d\vec{k}(2\pi)^{-3}L_{cv}(\omega)|L_{cv}(\omega)|^2=\mathcal{J}_0 I_1(E_G-\hbar\omega-i\gamma_{cv}) , \tag{A15b}$$

$$\int d\vec{k}(2\pi)^{-3}L_{vc}(\omega)|L_{cv}(\omega)|^2=\mathcal{J}_0 I_2(E_G+\hbar\omega+i\gamma_{cv},E_G-\hbar\omega+i\gamma_{cv}) , \tag{A15c}$$

$$\int d\vec{k}(2\pi)^{-3}L_{cv}(\omega)|L_{vc}(\omega)|^2=\mathcal{J}_0 I_2(E_G-\hbar\omega-i\gamma_{cv},E_G+\hbar\omega+i\gamma_{cv}) , \tag{A15d}$$

$$\int d\vec{k}(2\pi)^{-3}[L_{vc}(\omega)]^2=\mathcal{J}_0 I_3(E_G+\hbar\omega+i\gamma_{cv}) , \tag{A15e}$$

$$\int d\vec{k}(2\pi)^{-3}[L_{cv}(\omega)]^2=\mathcal{J}_0 I_3(E_G-\hbar\omega-i\gamma_{cv}) , \tag{A15f}$$

$$\int d\vec{k}(2\pi)^{-3}|L_{cv}(\omega)|^2=\mathcal{J}_0 I_4(E_G-\hbar\omega,\gamma_{cv}) , \tag{A15g}$$

$$\int d\vec{k}(2\pi)^{-3}|L_{vc}(\omega)|^2=\mathcal{J}_0 I_4(E_G+\hbar\omega,\gamma_{cv}) . \tag{A15h}$$

Collecting all of these together gives (7a) and (7b).

---

[1]R. K. Jain and M. B. Klein, Appl. Phys. Lett. 35B, 454 (1979).

[2]R. K. Jain, M. B. Klein, and R. C. Lind, Opt. Lett. 4, 328 (1979).

[3]R. K. Jain and D. G. Steel, Appl. Phys. Lett. 37, 1 (1980).

[4]M. A. Khan, P. W. Kruse, and J. F. Ready, Opt. Lett. 5, 261 (1980).

[5]David Depatie and Donald Haueisen, Opt. Lett. 5, 252 (1980).

[6]D. A. B. Miller, R. G. Harrison, A. M. Johnston, C. T. Seaton, and S. D. Smith, Opt. Commun. 32, 478 (1980).

[7]R. L. Abrams and R. C. Lind, Opt. Lett. 2, 94 (1978).

[8]A. Elci, D. Rogovin, D. Depatie, and D. Haueisen, J. Opt. Soc. Am. 70, 990 (1980).

[9]See, for example, D. Long, in *Semiconductors and Semimetals*, edited by R. K. Willardson and A. C. Beer (Academic, New York, 1966), Vol. I.

[10]P. A. Wolff and G. A. Pearson, Phys. Rev. Lett. 17, 1015 (1966).

[11]In adapting Eq. (2-8) of Ref. 8 for the absorption coefficient, one should note that since the crystal orientation and the light polarization are fixed, it should be multiplied by 3. The factor $\frac{1}{3}$ in the original formula comes from an angular average over atomic or molec-

ular orientation.

[12]For a specific example see A. Elci, M. Scully, J. Matter, and A. Smirl, Phys. Rev. B 16, 191 (1977).

[13]E. O. Kane, in *Semiconductors and Semimetals,* edited by R. K. Willardson and A. C. Beer (Academic, New York, 1966), Vol. I.

[14]W. Heitler, *Quantum Theory of Radiation* (Oxford University Press, London, 1960); p. 77. Note that the annihilation operator q_λ in this reference differs from b_λ by a normalization factor $(\hbar/2\omega_\lambda)^{1/2}$.

[15]T. S. Moss, G. J. Burrell, and B. Ellis, *Semiconductor Opto-electronics* (Butterworth, London, 1973).